Spatiotemporal variability of dissolved inorganic macronutrients along the northern Antarctic Peninsula

Thiago Monteiro[1,2,3*], Sian Henley[4], Ricardo César Gonçalves Pollery[5], Carlos Rafael Borges Mendes[2,6], Mauricio Mata[1,2], Virginia Maria Tavano[6], Carlos Alberto Eiras Garcia[1,2], and Rodrigo Kerr[1,2,3]

[1]Programa de Pós-Graduação em Oceanologia, Instituto de Oceanografia, Universidade Federal do Rio Grande (FURG), Av. Itália km 8, Rio Grande, 96203-900, RS, Brazil.

[2]Laboratório de Estudos dos Oceanos e Clima, Instituto de Oceanografia, Universidade Federal do Rio Grande (FURG), Av. Itália km 8, Rio Grande, 96203-900, RS, Brazil.

[3]Brazilian Ocean Acidification Network (BrOA), Rio Grande, 96203-900, RS, Brazil.

[4]School of GeoSciences, University of Edinburgh, Edinburgh, EH9 3FE, United Kingdom.

[5]Unidade Multiusuário de Análises Ambientais, Centro de Ciências da Saúde, Universidade Federal do Rio de Janeiro (UFRJ), Cidade Universitária, 21941-902 Rio de Janeiro, Brazil.

[6]Laboratório de Fitoplâncton e Microorganismos Marinhos, Instituto de Oceanografia, Universidade Federal do Rio Grande (FURG), Av. Itália, km 8, Rio Grande, RS, Brazil.

Supplementary information
The file contains:

Figure S1 to Figure S8
Table S1
Table S2

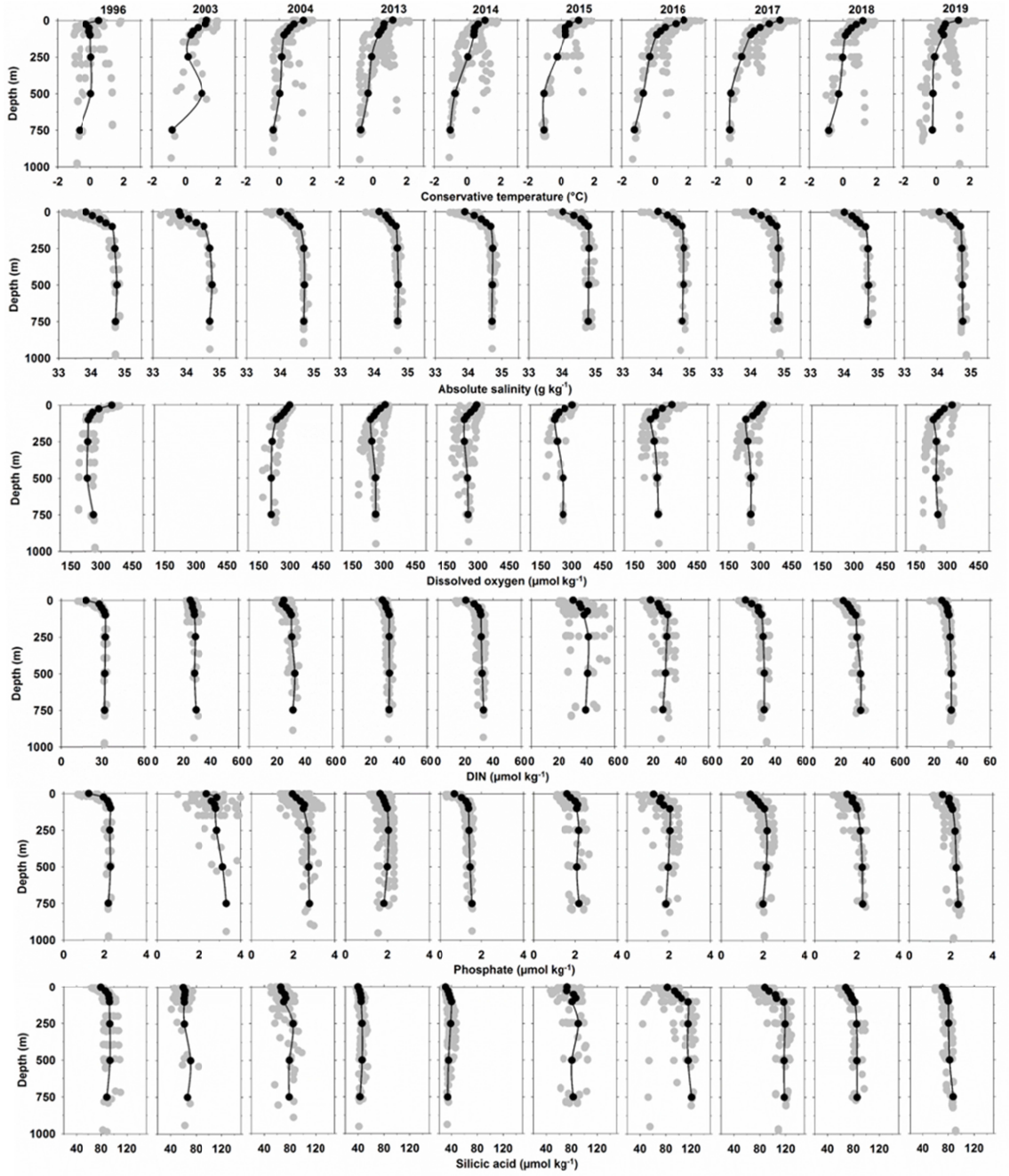

Figure S1: The gray dots show the profiles of hydrographic parameters and macronutrients sampled in the austral summer along the Gerlache Strait from 1996 to 2019 and the black dots show the average profiles of each property, used to compose figures 4 and 5 in the main text.

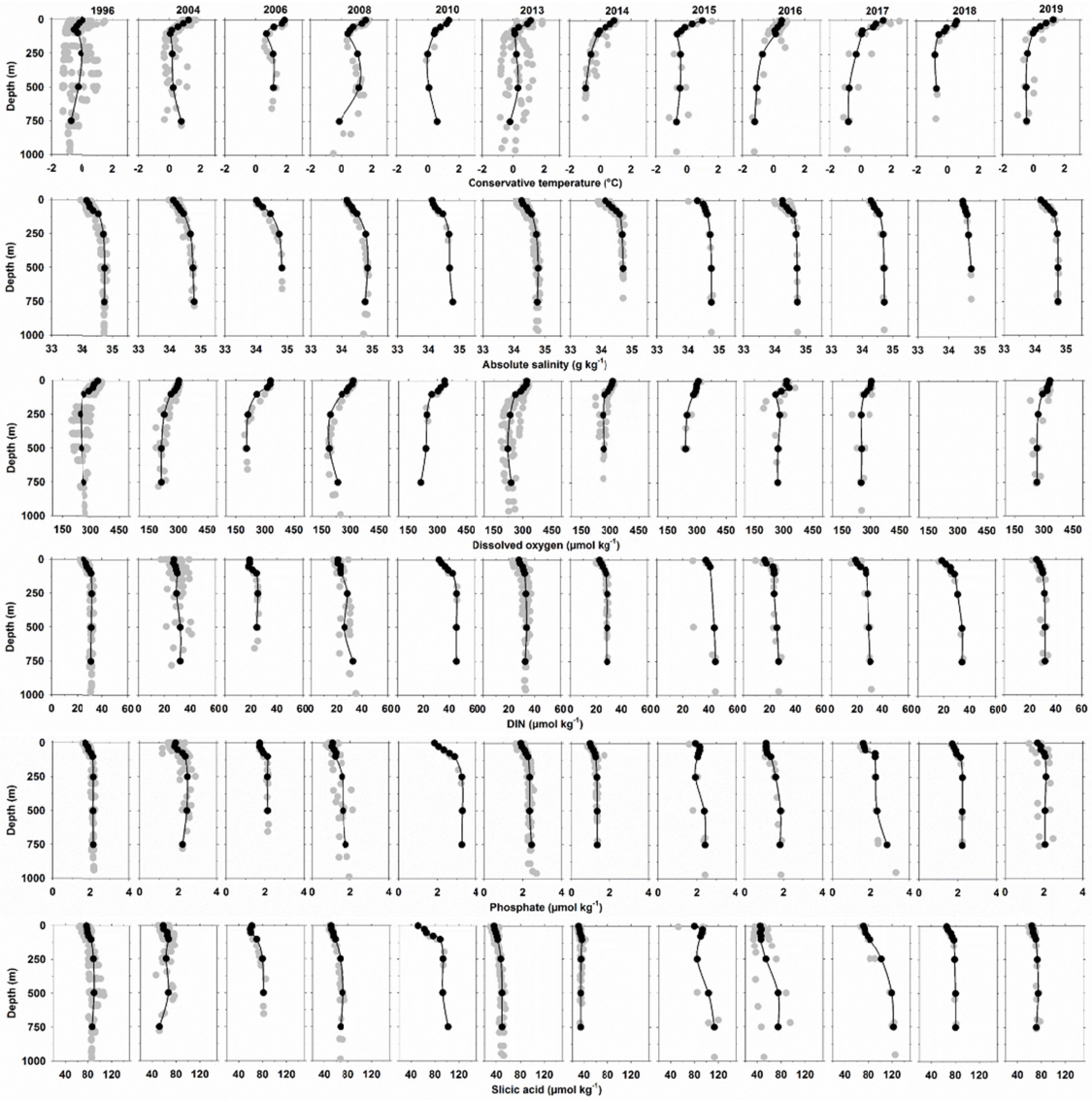

Figure S2: The gray dots show the profiles of hydrographic parameters and macronutrients sampled in the austral summer along the western basin of the Bransfield Strait from 1996 to 2019 and the black dots show the average profiles of each property, used to compose figures 4 and 5 in the main text.

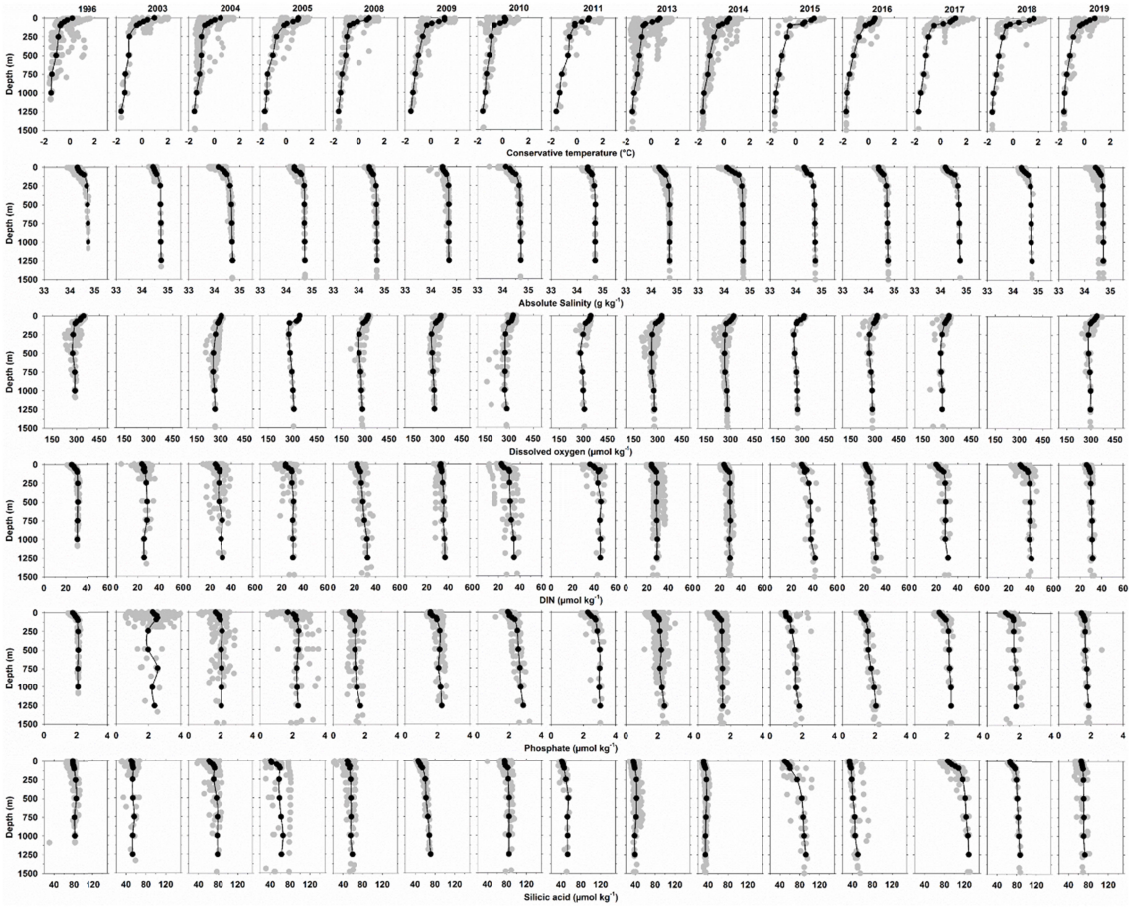

Figure S3: The gray dots show the profiles of hydrographic parameters and macronutrients sampled in the austral summer along the central basin of the Bransfield Strait from 1996 to 2019 and the black dots show the average profiles of each property, used to compose figures 4 and 5 in the main text.

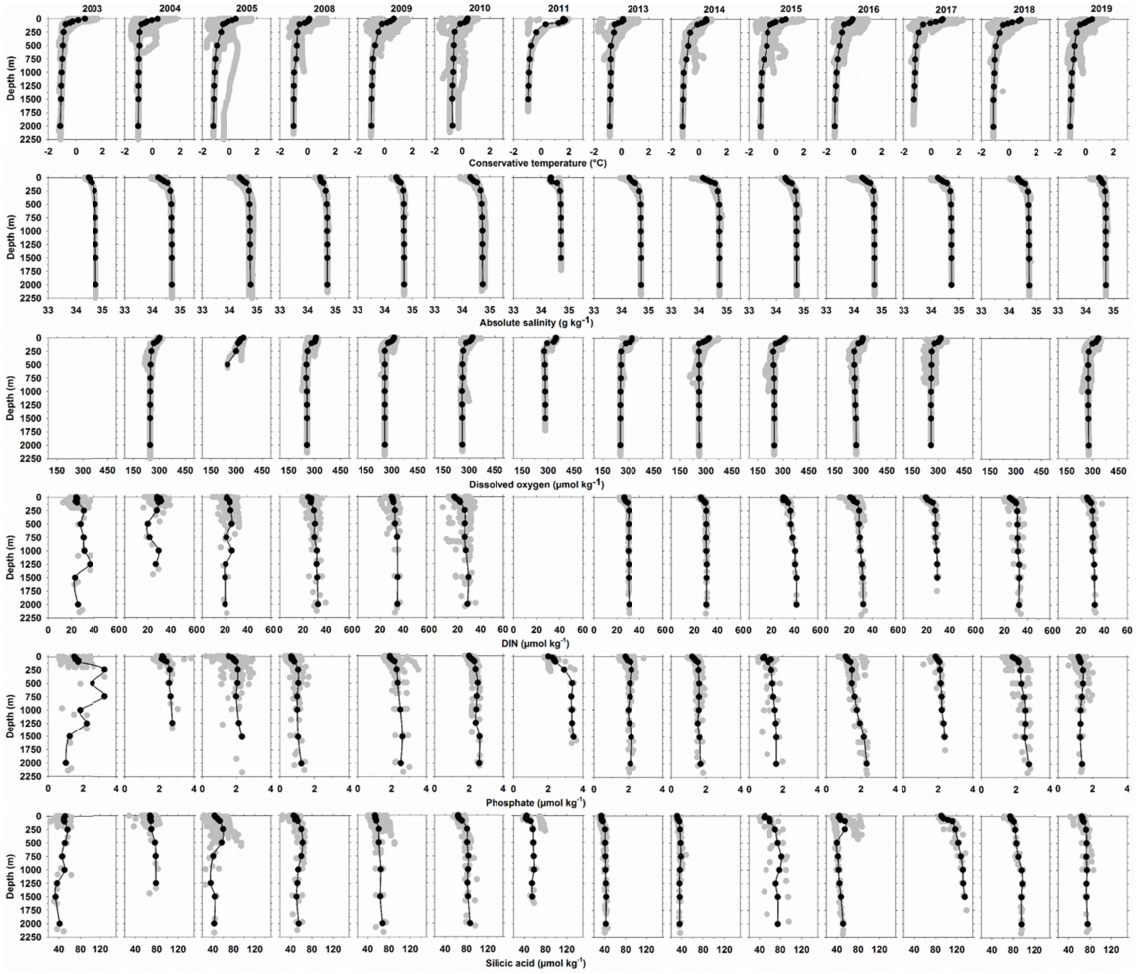

Figure S4: The gray dots show the profiles of hydrographic parameters and macronutrients sampled in the austral summer along the eastern basin of the Bransfield Strait from 1996 to 2019 and the black dots show the average profiles of each property, used to compose figures 4 and 5 in the main text.

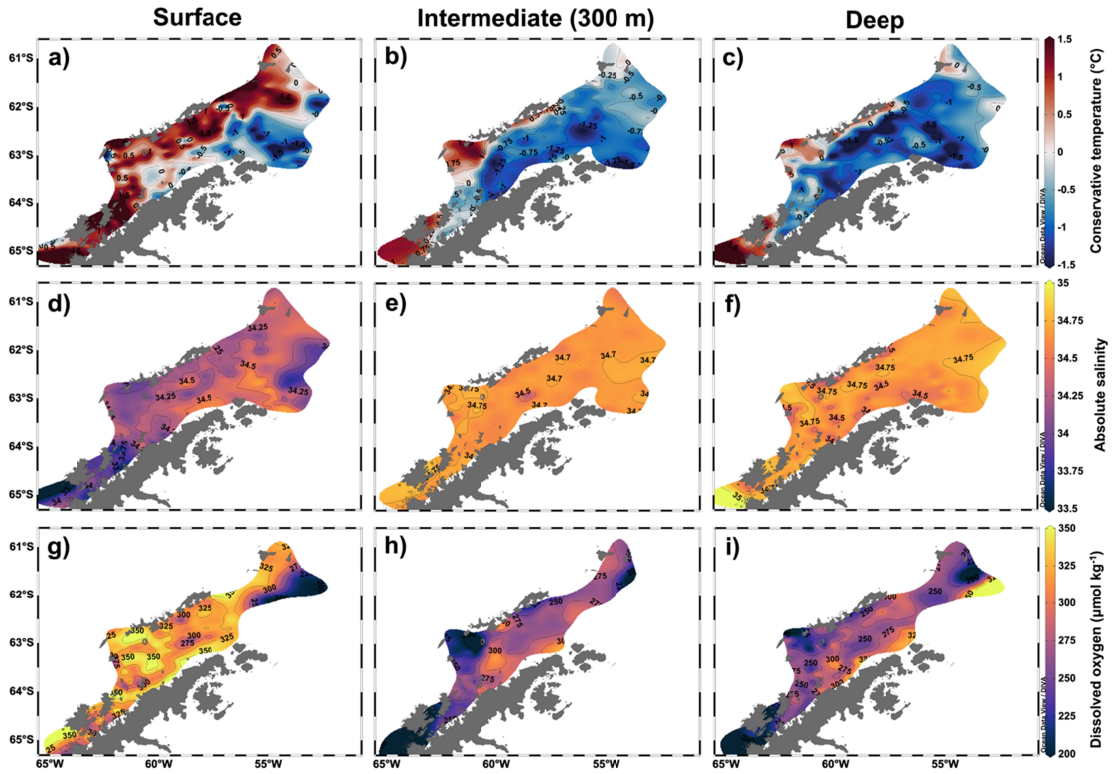

Figure S5: Surface (up to 5m), intermediate (at 300m) and deep spatial distribution of (a-c) conservative temperature, (d-f) absolute salinity, and (g-i) dissolved oxygen during austral summer (Jan-Mar) along the northern Antarctic Peninsula from 1996 to 2019.

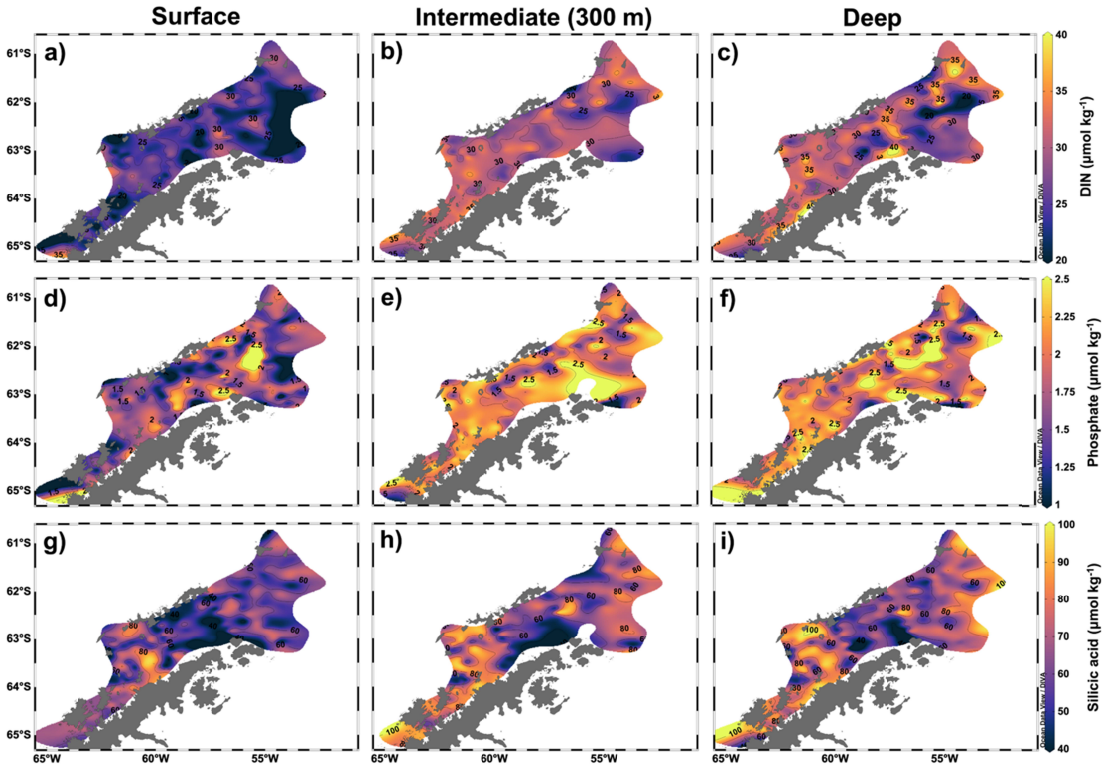

Figure S6: Surface (up to 5m), intermediate (at 300m) and deep spatial distribution of (a-c) dissolved inorganic nitrogen (DIN), (d-f) phosphate, and (g-i) silicic acid during austral summer (Jan-Mar) along the northern Antarctic Peninsula from 1996 to 2019.

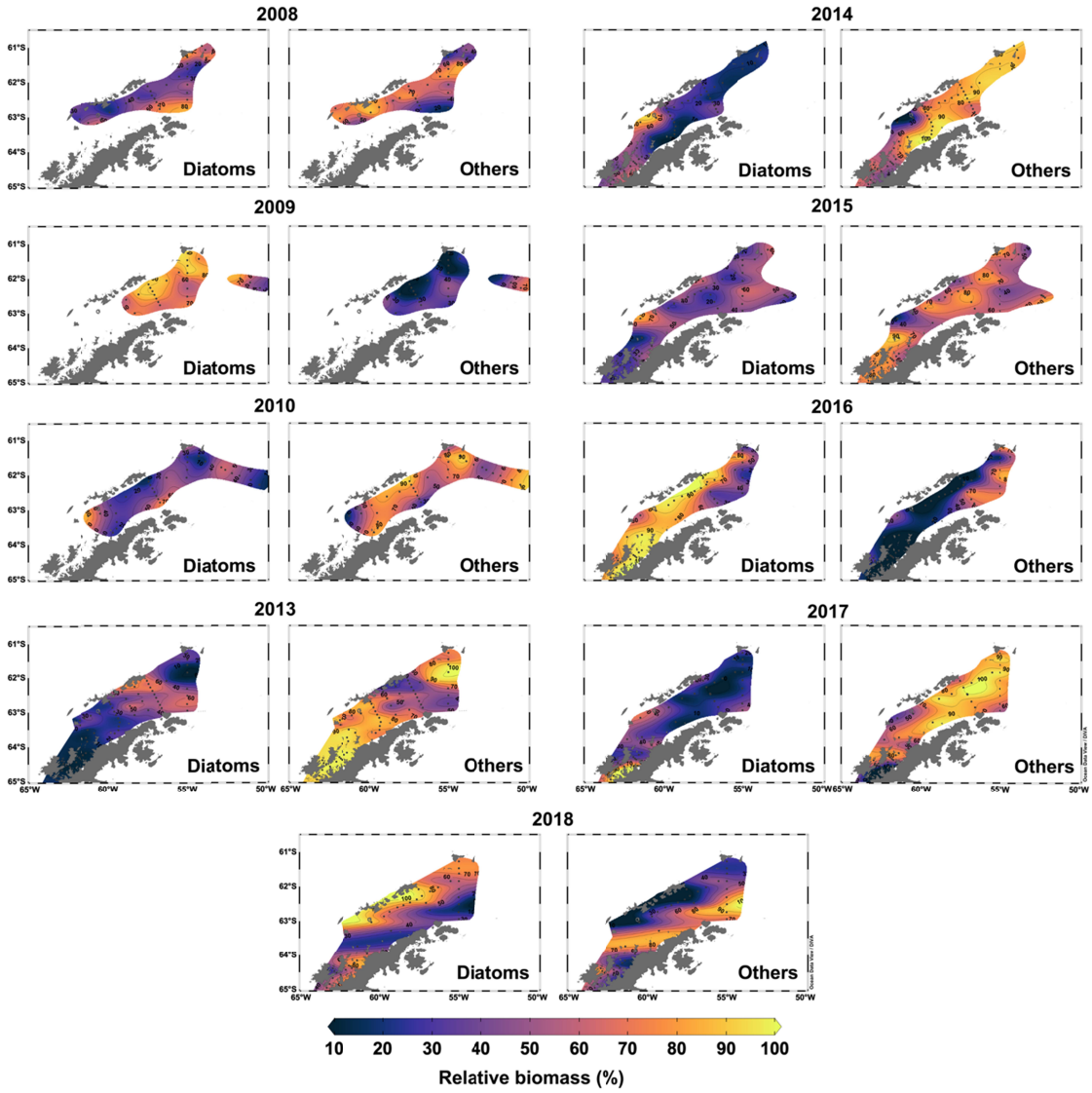

Figure S7: Percentage of relative phytoplankton biomass during austral summer along the northern Antarctic Peninsula from 2008 to 2018. Here we separate the phytoplankton composition between diatoms and other smaller groups (Dinoflagellates, Phaeocystis, Cryptophytes, and green flagellates). All analyses of the composition of phytoplankton groups used here are detailed in Costa et al. (2020, 2021 and references therein).

Table S1: Sign of the SAM and ENSO indices in the respective sampling years along the NAP. The SAM and ENSO indices refer to 4 and 6 months prior to the sampling month, respectively.

Year	Sampling month	SAM	ENSO
1996	January	+	-
2003	January	-	+
2004	January	+	+
2005	January	-	+
2006	March	+	-
2008	February	-	-
2009	February	+	-
2010	March	+	+
2011	March	+	-
2013	February	-	+
2014	February	-	-
2015	February	+	+
2016	February	-	+
2017	February	+	-
2018	February	+	-
2019	January	+	+

Table S2: DIN/phosphate and silicic acid/DIN regression statistics for the summer profiles in each year along the northern Antarctic Peninsula. The ratios ± the standard deviations are the slope and root mean square error from the regressions, respectively.

	Year	Gerlache Strait	Western Bransfield	Central Bransfield	Eastern Bransfield
DIN/P statistics	1996	13.38 ± 0.59 (R^2=0.99; p<0.001; n=8)	15.66 ± 0.46 (R^2=0.99; p<0.001; n=8)	16.24 ± 0.40 (R^2=0.99; p<0.001; n=9)	
	2003	3.94 ± 1.07 (R^2=0.69; p=0.010; n=8)			
	2004	10.28 ± 1.59 (R^2=0.88; p<0.001; n=8)	7.21 ± 1.53 (R^2=0.82; p=0.005; n=7)	12.69 ± 3.67 (R^2=0.63; p=0.011; n=9)	
	2005			11.86 ± 2.69 (R^2=0.71; p=0.002; n=10)	6.44 ± 3.07 (R^2=0.42; p<0.081; n=8)
	2006		15.25 ± 2.36 (R^2=0.91; p=0.003; n=6)		
	2008		14.4 ± 2.10 (R^2=0.89; p<0.001; n=8)	15.62 ± 2.74 (R^2=0.80; p<0.001; n=10)	13.12 ± 1.94 (R^2=0.84; p<0.001; n=11)
	2009			5.64 ± 0.79 (R^2=0.86; p<0.001; n=10)	6.76 ± 0.49 (R^2=0.97; p<0.001; n=9)
	2010		9.57 ± 0.23 (R^2=0.99; p<0.001; n=8)	11.68 ± 1.30 (R^2=0.91; p<0.001; n=10)	19.77 ± 1.31 (R^2=0.96; p<0.001; n=11)
	2011			11.35 ± 1.71 (R^2=0.86; p<0.001; n=9)	
	2013	12.19 ± 2.62 (R^2=0.78; p=0.003; n=8)	10.19 ± 1.35 (R^2=0.90; p<0.001; n=8)	9.38 ± 1.59 (R^2=0.81; p<0.001; n=10)	13.57 ± 1.87 (R^2=0.84; p<0.001; n=12)
	2014	15.09 ± 0.41 (R^2=0.99; p<0.001; n=8)	17.46 ± 0.71 (R^2=0.99; p<0.001; n=7)	12.77 ± 0.79 (R^2=0.97; p<0.001; n=10)	11.58 ± 1.19 (R^2=0.90; p<0.001; n=12)
	2015	17.25 ± 2.46 (R^2=0.89; p<0.001; n=8)	14.95 ± 2.02 (R^2=0.95; p=0.005; n=6)	12.74 ± 1.01 (R^2=0.95; p<0.001; n=10)	12.81 ± 1.33 (R^2=0.94; p<0.001; n=8)
	2016	14.41 ± 1.15 (R^2=0.96; p<0.001; n=8)	9.00 ± 2.96 (R^2=0.61; p=0.023; n=8)	10.89 ± 0.71 (R^2=0.97; p<0.001; n=10)	8.78 ± 1.19 (R^2=0.85; p<0.001; n=12)
	2017	16.30 ± 2.02 (R^2=0.92; p<0.001; n=8)	9.62 ± 1.31 (R^2=0.90; p<0.001; n=8)	13.70 ± 1.00 (R^2=0.96; p<0.001; n=10)	21.60 ± 2.41 (R^2=0.90; p<0.001; n=11)
	2018	16.74 ± 1.37 (R^2=0.97; p<0.001; n=7)	24.80 ± 2.96 (R^2=0.93; p<0.001; n=7)	16.01 ± 0.91 (R^2=0.91; p<0.001; n=10)	8.84 ± 1.05 (R^2=0.88; p<0.001; n=12)
	2019	9.40 ± 0.87 (R^2=0.95; p<0.001; n=8)	13.72 ± 1.82 (R^2=0.82; p<0.001; n=7)	13.09 ± 0.94 (R^2=0.94; p<0.001; n=10)	20.29 ± 2.71 (R^2=0.90; p<0.001; n=8)

	Year	Gerlache Strait	Western Bransfield	Central Bransfield	Eastern Bransfield
Silicic acid/DIN statistics	1996	0.97 ± 0.14	1.8 ± 0.35	1.04 ± 0.25	
		(R^2=0.89; p<0.001; n=8)	(R^2=0.82; p=0.002; n=8)	(R^2=0.71; p=0.004; n=9)	
	2003	1.31 ± 0.96		0.81 ± 0.23	3.07 ± 0.47
		(R^2=0.24; p=0.223; n=8)		(R^2=0.64; p=0.010; n=8)	(R^2=0.84; p<0.001; n=10)
	2004	1.63 ± 0.50	1.73 ± 0.57	2.65 ± 0.37	
		(R^2=0.64; p=0.017; n=8)	(R^2=0.70; p=0.039; n=6)	(R^2=0.87; p<0.001; n=9)	
	2005			2.74 ± 0.30	3.69 ± 0.80
				(R^2=0.91; p<0.001; n=10)	(R^2=0.84; p<0.010; n=8)
	2006		2.78 ± 0.55		
			(R^2=0.86; p=0.007; n=6)		
	2008		1.54 ± 0.40	0.84 ± 0.16	3.02 ± 0.36
			(R^2=0.71; p=0.009; n=8)	(R^2=0.78; p<0.001; n=10)	(R^2=0.92; p<0.001; n=8)
	2009			5.55 ± 0.46	2.61 ± 0.26
				(R^2=0.95; p<0.001; n=10)	(R^2=0.93; p<0.001; n=9)
	2010		3.21 ± 0.25	0.88 ± 0.13	2.03 ± 0.18
			(R^2=0.97; p<0.001; n=8)	(R^2=0.84; p<0.001; n=10)	(R^2=0.93; p<0.001; n=11)
	2011			1.18 ± 0.31	
				(R^2=0.68; p=0.006; n=9)	
	2013	1.02 ± 0.23	2.33 ± 0.42	0.84 ± 0.22	2.01 ± 0.20
		(R^2=0.76; p=0.005; n=8)	(R^2=0.83; p=0.002; n=8)	(R^2=0.64; p=0.006; n=10)	(R^2=0.91; p<0.001; n=12)
	2014	0.65 ± 0.17	0.65 ± 0.17	0.91 ± 0.12	1.15 ± 0.17
		(R^2=0.75; p=0.012; n=7)	(R^2=0.76; p=0.002; n=8)	(R^2=0.88; p<0.001; n=10)	(R^2=0.82; p<0.001; n=12)
	2015	1.34 ± 0.40	3.83 ± 0.68	4.03 ± 0.38	4.05 ± 0.49
		(R^2=0.66; p=0.015; n=8)	(R^2=0.91; p<0.011; n=5)	(R^2=0.93; p<0.001; n=10)	(R^2=0.90; p<0.001; n=12)
	2016	3.09 ± 0.57	1.73 ± 1.17	1.56 ± 0.16	1.36 ± 0.18
		(R^2=0.83; p=0.002; n=8)	(R^2=0.31; p=0.197; n=7)	(R^2=0.92; p<0.001; n=10)	(R^2=0.86; p<0.001; n=12)
	2017	2.45 ± 0.22	3.97 ± 1.07	4.15 ± 0.34	4.34 ± 0.25
		(R^2=0.95; p<0.001; n=8)	(R^2=0.70; p=0.01; n=8)	(R^2=0.95; p<0.001; n=10)	(R^2=0.97; p<0.001; n=11)
	2018	1.53 ± 0.12	1.02 ± 0.11	1.89 ± 0.19	2.97 ± 0.46
		(R^2=0.97; p<0.001; n=7)	(R^2=0.95; p<0.001; n=7)	(R^2=0.92; p<0.001; n=10)	(R^2=0.81; p<0.001; n=12)
	2019	2.01 ± 0.31	1.67 ± 0.20	1.24 ± 0.11	1.67 ± 0.17
		(R^2=0.87; p<0.001; n=8)	(R^2=0.93; p<0.001; n=7)	(R^2=0.95; p<0.001; n=10)	(R^2=0.91; p<0.001; n=12)